Synthesis and characterization of a photoaffinity labelling probe based on the structure of the cystic fibrosis drug ivacaftor

C. Michael Hamilton,[†] Maurita Hung,[‡] Gang Chen,[†] Zafar Qureshi,[†] John R. Thompson,[†] Bingyun Sun,[†] Christine E. Bear,[‡] Robert N. Young.*[,†#]

[†]Department of Chemistry, Simon Fraser University, Burnaby, BC, Canada

[‡] Molecular Medicine, The Hospital for Sick Children, Toronto, ON, Canada

[#]This manuscript is dedicated to the fond memory of Sir Derek H. R. Barton on the occasion of the centenary of his birth.

Final version available as:

Hamilton, C. M., Hung, M., Chen, G., Qureshi, Z. & Thompson, J. R., Sun, B., Bear, C. E., Young, R. N.(2018). Synthesis and characterization of a photoaffinity labelling probe based on the structure of the cystic fibrosis drug ivacaftor. *Tetrahedron*. 10.1016/j.tet.2018.06.016.

*Author to whom correspondence should be addressed

Tel: +1(778) 782-3351

Fax: +1(778) 782-3765

e-mail: robert_young@sfu.ca

ABSTRACT:

Cystic Fibrosis (CF) is a genetic disorder caused by loss-of-function mutations to the gene encoding the cystic fibrosis transmembrane conductance regulator (CFTR) protein. Ivacaftor (**1**) was the first therapeutic approved for the treatment of CF that is able to restore gating activity to certain CFTR variants although the mechanism of action is poorly understood. Herein we describe the synthesis of a photoaffinity labelling (PAL) probe (**2**) based on the structure of ivacaftor incorporating a photoreactive diazirine moiety for use in labelling studies designed to identify the binding site for ivacaftor on mutant CFTR. The PAL probe **2** retained potentiation activity, with a potency similar to **1**, using a Fluorescent Imaging Plate Reader (FLIPR®) assay measuring ion conductance potentiation of wild type (Wt)-CFTR. Photolabelling experiments with human serum albumin (HSA) as a model protein have shown that probe **2** can label HSA in a manner consistent with observed and predicted binding.

Graphical Abstract:

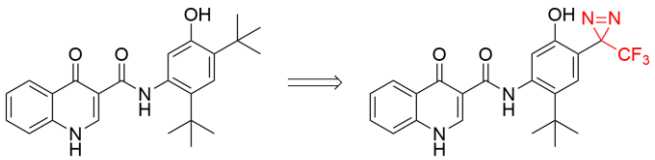

Ivacaftor (**1**) Photoprobe (**2**)

1. Introduction

Cystic fibrosis (CF) is an autosomal recessive disorder and the most common fatal genetic disease affecting North Americans.[1,2] The underlying cause of CF results from loss-of-function mutations in the gene encoding the cystic fibrosis transmembrane conductance regulator protein (CFTR).[3–5] Wild-type CFTR is a phosphorylation dependent nucleotide regulated ion channel primarily responsible for the flux of chloride and bicarbonate across the apical membranes of epithelial tissues.[6] For individuals with CF, loss of CFTR activity results in dysregulation of ion flux and extracellular fluid composition.[7] CF affects

many organs in the body including the pancreas, gastrointestinal tract, reproductive system, liver, skin, and lungs. Loss of CFTR function in the lungs, the organ most overtly affected, leads to dehydration of the airway surface fluid causing mucus plugging, a propensity for bacterial infection, inflammation, bronchiectasis and eventually respiratory failure.

Historically, disease management for CF primarily focused on treating the resulting symptoms including the use of antibiotics to combat chronic respiratory infections, aerosolised mucolytics to reduce mucus plugging and enzyme administration to aid in digestion and nutrient uptake.[8] With the recent development and clinical implementation of CFTR modulating small-molecule therapies, clinicians are now able to treat the underlying cause of the disease.[9] Many classes of CFTR modulators have been described and have undergone clinical testing. The first FDA approved CFTR modulator, ivacaftor (**1**), is termed a CFTR "potentiator" as it restores gating to CFTR protein which has been successfully trafficked to the cell membrane. Ivacaftor was discovered through the use of high-throughput functional screening followed by an extensive medicinal chemistry program.[10] As a result, the exact mechanism of action is not yet fully understood, including the location of the binding site(s) on mutant CFTR. Understanding the interactions between **1** and mutant CFTR will provide insights useful in the development of new therapeutically useful compounds.

One method for identifying the location of the binding site of a compound on its target protein is through the use of a photo-affinity labelling (PAL) probe.[11] Generating a PAL probe involves the incorporation of a photoreactive group onto the compound of interest, which upon irradiation forms a highly reactive species that can covalently bind to proximal amino acid residues in the binding site. An important aspect of generating a PAL probe is to ensure that incorporation of the reactive moiety does not significantly alter the affinity of the probe for the target protein relative to the parent compound. The most common photoreactive groups used in PAL probes are the diazirine,[12] azide,[13] and benzophenone moieties.[14,15] Each of these groups have different properties, including activation wavelength, nature and half-life of reactive species produced, reagent stability, size, lipophilicity, and propensity to rearrange. Additionally, PAL probes commonly feature a reporter tag to aid in the identification and isolation of labelled proteins,

including secondary targets for the compound of interest.[11] A variety of reporter tags can be utilized; such as radiolabels, fluorophores, biotin; or a latent group (such as an acetylene) that can be reacted with a tagging molecule via click chemistry following the photolabelling event. In recent years the diazirine has become a favoured choice of photoreactive group as it is stable to a wide range of reaction conditions, activated by a wavelength of light which does not significantly affect proteins or DNA (365 nm) and produces a very reactive singlet carbene which has a short half-life and can insert into N-H, C-H, and O-H bonds.[16,17]

Towards the goal of elucidating the binding site of **1** on mutant CFTR, we have synthesized PAL probe **2**, featuring a diazirine moiety, based on the ivacaftor scaffold. Herein, we discuss the design and synthesis of **2**, as well as initial characterization of its stability, photoreactivity, and functional activity on the CFTR channel. We have demonstrated the ability of **2** to efficiently label human serum albumin (HSA), a protein that has been previously reported to have a strong affinity for **1**.[18]

2. Results and discussion

2.1. Retrosynthetic analysis

In generating PAL probe **2**, it was important to ensure that the installation of the photoreactive group would not significantly alter the binding affinity and bioactivity compared to ivacaftor. It has been shown that modifications to either of the two *t*-butyl groups on the scaffold could be tolerated with retention of CFTR potentiating activity.[10] Modification of the *t*-butyl group *ortho* to the phenolic moiety affected the potentiation EC_{50} to a greater degree than did changes to the *para*-*t*-butyl, suggesting that the *ortho* group might have a closer interaction with the surface of the binding site on CFTR.[10] Considering the similar size and lipophilicity of a diazirine moiety compared to a *t*-butyl group, we envisaged a target PAL probe where a diazirine motif replaces the *t*-butyl group *ortho* to the phenolic moiety, and thus the molecule **2** was chosen as our target PAL probe.

Retrosynthetic analysis of compound **2** suggested two possible synthetic routes (**Figure 1**). The first involved forming an amide bond between carboxylic acid **A** (potentially substituted with a reporter tag),

and an aniline **B** containing the diazirine moiety. **B** could be prepared from **D** where the diazirine group would be installed via manipulation of a synthetic handle such as X = Br or I. The second route reversed this process, forming the amide bond between aniline **D** and acid **A** to give compound **C**, followed by installation of the diazirine group (**Figure 1**).

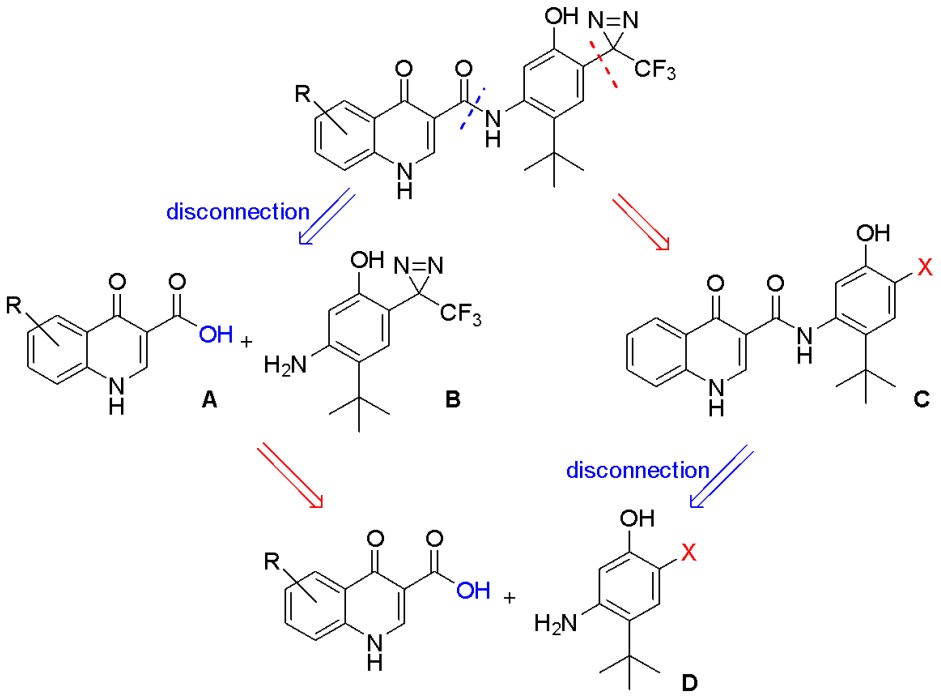

Figure 1. Retrosynthetic analysis of routes of synthesis of the diazirine-containing PAL probe (R indicates potential attachment of a reporter tag)

*2.2. Synthesis of PAL probe **2***

Initial synthetic efforts focused on the first route and synthesis of **B** (compound **3**). The synthesis of **3** **(Scheme 1)** began from known phenol **4** with the reaction with chloromethyl ethyl ether to give **5**.[19] Selective reduction of the nitro group in **5** proceeded smoothly with iron and ammonium chloride to give aniline **6**, and subsequent protection of the aniline with di-*t*-butyl dicarbonate (Boc_2O) gave **7**. Installation of the trifluoromethyl ketone was achieved by first deprotonation of the amide NH with MeLi, followed by lithium-halogen exchange using *n*-BuLi, and quenching the resulting di-anion with ethyl trifluoroacetate to provide trifluoromethyl ketone **8** in excellent yield (95%). Compound **8** was reacted with hydroxylamine hydrochloride in a 2:1 pyridine/methanol mixture to give a mixture of *E,Z* isomers of oxime **9** in a 2:1 ratio

(stereochemistry undetermined). Reaction of oximes **9** with *p*-toluenesulphonyl chloride gave tosyl-oximes **10** which were subsequently treated with liquid ammonia in a sealed vessel to give diaziridine **11.** Upon close inspection, the crude reaction mixture was found to be a 2.7:1 mixture of an amidine by-product **12** and the desired diaziridine **11**. Separation of **12** and isolation of pure **11** could be performed at this stage by either semi-preparative HPLC or selective crystallization, but this was somewhat demanding and low yielding. The identity of this side product **12** was unambiguously confirmed by single crystal X-ray diffraction (**Scheme 1**, Supplementary Information **Figure S1**). A better overall yield of the final product (the diazirine **13**) and easier separation was achieved by carrying the mixture of **11** and **12** into the next step. Oxidation of the mixture of **11** and **12** with iodine and trimethylamine in methanol smoothly gave **13** (along with unchanged amidine **12**), which was easily obtained pure via silica chromatography (shielded from light). The deprotection of **13** with methanolic hydrogen chloride produced the desired aniline **3**; however, this species was found to be very reactive with a short half-life, quickly forming adducts with solvent. Nonetheless, with **3** in hand, amide coupling reactions with 4-oxo-1,4-dihydroquinoline-3-carboxylic acid (**14**) were attempted under a variety of conditions, but all attempts resulted in loss of the diazirine and production of products of decomposition of the diazirine. Unfortunately, despite extreme precautions to exclude light, the aniline **3** proved to be too unstable to survive the relatively slow amide bond forming reactions with **14** and thus this approach was abandoned.

Scheme 1. Synthesis of diazirine **3**[a]

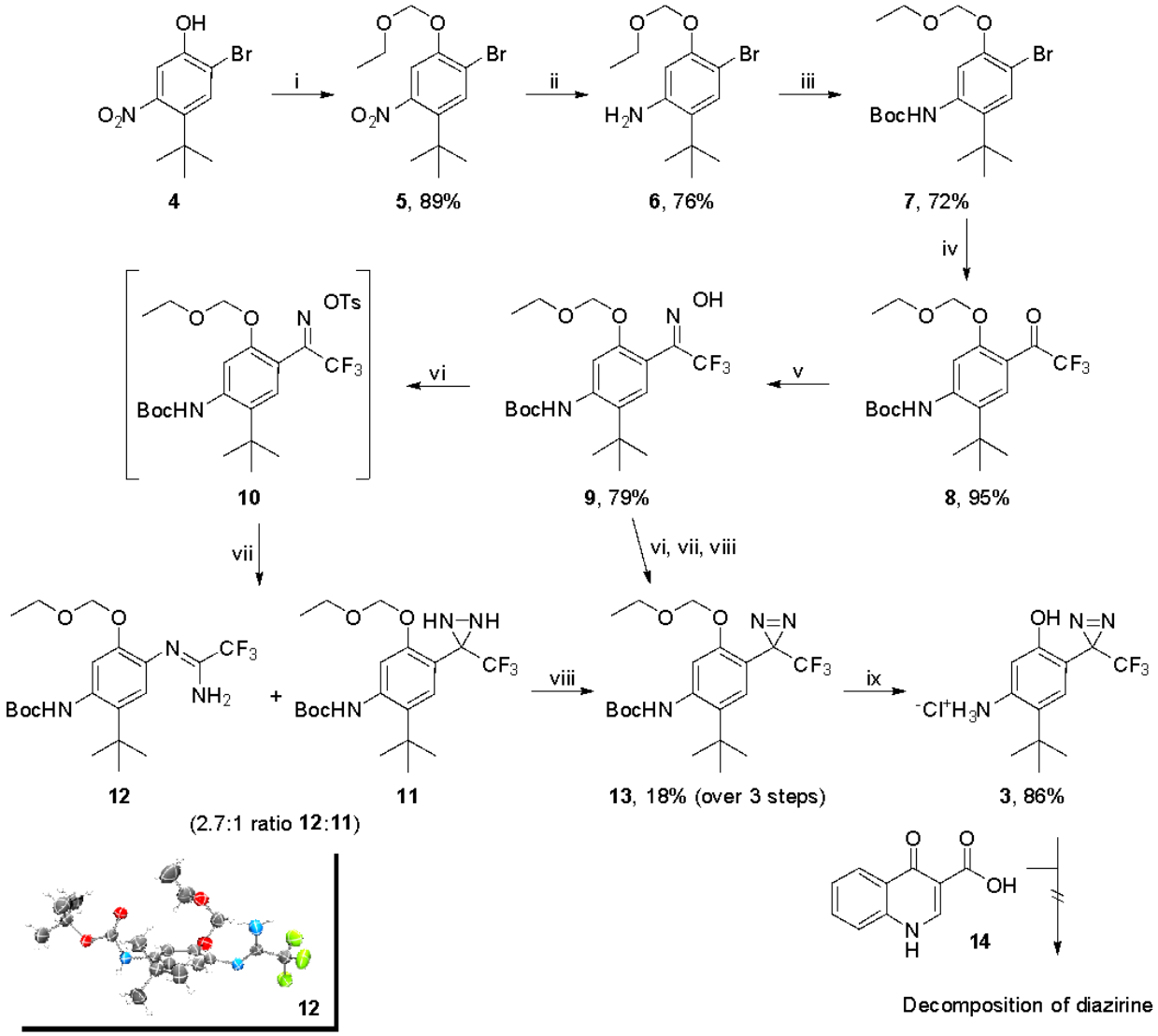

[a]Reagents and conditions: (i) Chloromethyl ethyl ether, DIPEA, THF, rt; (ii) Fe, NH_4Cl, MeOH, 60 °C; (iii) Boc_2O, Toluene, 105 °C, Microwave; (iv) a) MeLi, THF, -40 °C to rt, b) *n*-BuLi, THF, -78 °C, c) ethyl trifluoroacetate, -78 °C to rt; (v) $HONH_3 \cdot Cl$, 2:1 pyridine/MeOH, 65 °C, 18 h; (vi) TsCl, DIPEA, DCM, 0 °C to rt; (vii) NH_3 (l), DCM, 18 h, -78 °C to rt; (viii) I_2, Et_3N, MeOH, 18 h; (ix) HCl (g) MeOH.

Although we were unable to couple **3** with **14** with retention of the diazirine, we wanted to confirm that the photolytic decomposition of the diazirine group in the protected precursor **13** proceeded as expected. Thus, a solution of diazirine **13** in methanol was irradiated with UV light (365 nm) and the methanol photo-adduct **15** was isolated in excellent yield (**Scheme 2**). Notably, while **3** was very unstable, **13** was found to

be much less sensitive to light and we therefore surmised that installation of the diazirine after amide formation would have a greater chance of success.

Scheme 2. Photoreaction of diazirine **13** with MeOH

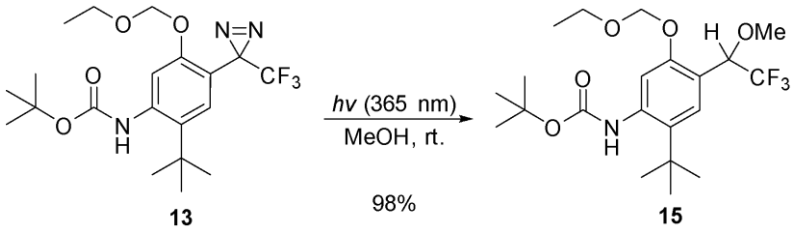

We therefore turned our attention to the alternative synthetic route (**Figure 1**, path B) where the two halves of the molecule were coupled at an early stage and the diazirine installed later as shown in **Scheme 3**. Coupling of aniline **6** and acid **14** with HATU gave bromo-amide **16** in good yield on multi-gram scale. Lithium-halogen exchange of the bromine atom in **16** was achieved by first addition of 2 equiv of MeLi to remove the NH protons followed by treatment with *n*-BuLi to generate a tri-anion species, which upon reaction with ethyl trifluoroacetate produced trifluoromethyl ketone **17**. Trifluoromethyl ketone **17** was isolated as a mixture of ketone and hydrate or hemi-ketal forms. At this stage, pure ketone **17** could be isolated by preparative-scale high-pressure liquid chromatography (prep-HPLC) in the absence of alcoholic solvents but only in low yields. However, carrying the original mixture forward directly into reaction with hydroxylamine hydrochloride gave the oximes **18** in better overall yield. In this way **18** could be isolated in 53% yield for the two steps as a mixture of *E/Z* isomers (2:1 ratio, undefined) by precipitation from DCM and without need for chromatography. Conversion of oximes **18** to the corresponding tosylate and formation of diaziridine **19** was carried out as a two-step, one-pot procedure. After reaction of **18** with *p*-toluenesulphonyl chloride in DCM, the reaction mixture was transferred to a reaction vessel containing condensed liquid ammonia and sealed at -40 ^{o}C and then allowed to react while warming to room temperature to give a mixture of diaziridine **19** and amidine **20** in a 2.6:1 ratio. Pure diaziridine **19** was successfully isolated by preparative reverse-phase HPLC. Diaziridine oxidation proceeded smoothly with Dess-Martin periodinane (DMP) to give diazirine **21**, and final deprotection with

methanolic HCl gave our target diazirine **2**. Gratifyingly, **2** did not require further purification and was stable for up to a year when stored cold (-20 °C) in the dark as either a solid or as a solution in DMSO.

Scheme 3. Synthesis of PAL probe **2**[a]

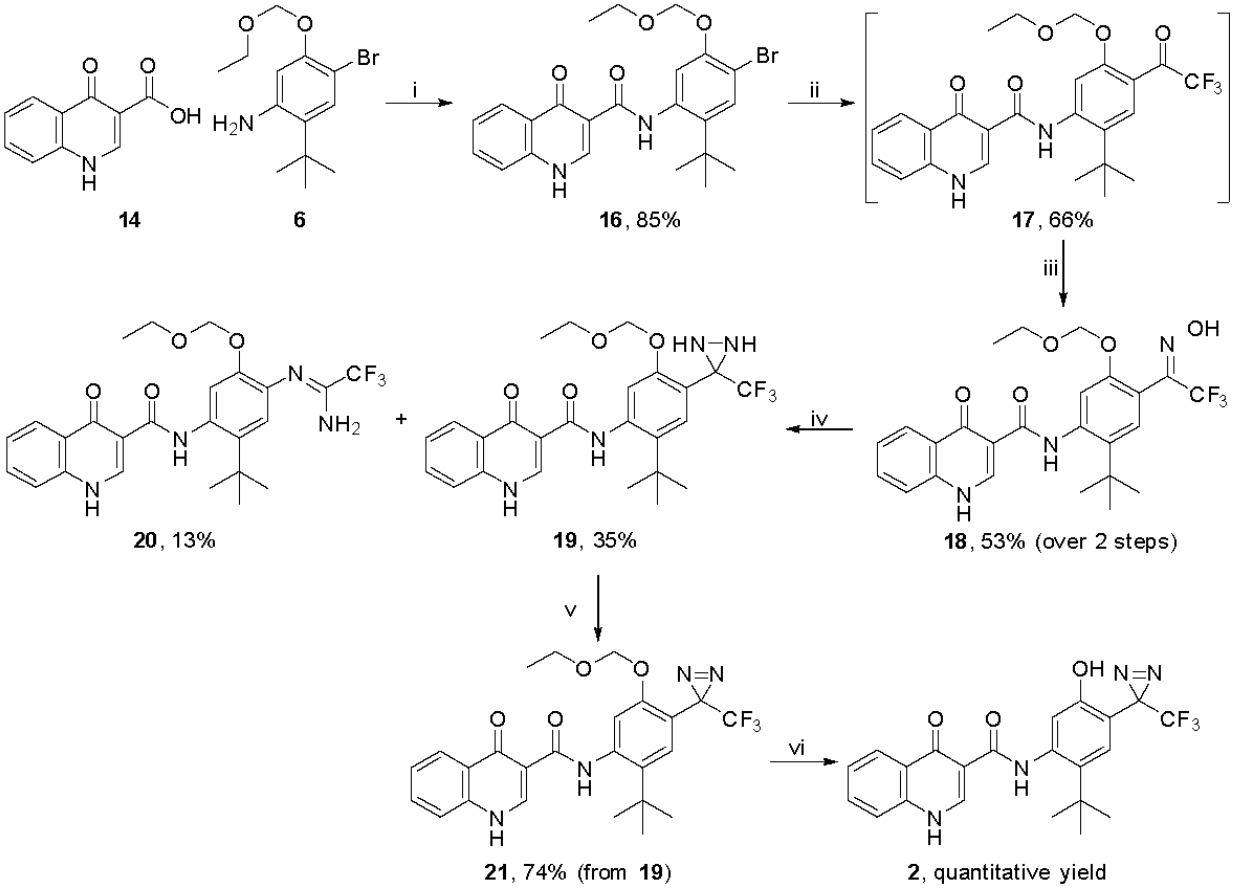

[a]Reagents and conditions: (i) HATU, HOBt, DIPEA, DMAP, DMF, 60 °C, 18h; (ii) a) MeLi, THF, -40 °C; b) *n*-BuLi, THF, -78 °C; c) ethyl trifluoroacetate, -78 °C to rt; (iii) $HONH_2 \cdot HCl$, 2:1 pyridine/MeOH, 60 °C, 18 h; (iv) a) TsCl, DIPEA, DCM, 0 °C to rt; b) NH_3 (*l*), DCM, 18 h, -40 °C to rt; (v) Dess-Martin periodinane, DCM, 2 h; (vi) HCl (*g*), MeOH.

A solution of diazirine **2** in methanol was irradiated with UV light (365 nm) (**Scheme 4**) and monitored by HPLC and LC-MS which after 3 hours showed essentially complete conversion to the methanol adduct **22**.

Scheme 4. Photoreaction of **2** with MeOH

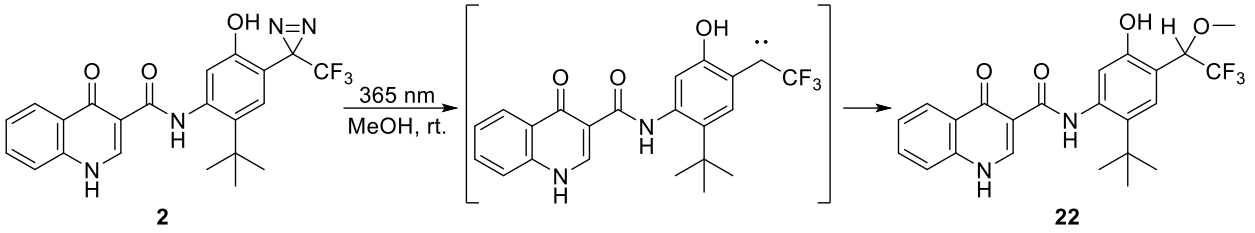

2 **22**

*2.3. Protein labelling and biological evaluation of photoaffinity probe **2***

To develop conditions for labelling proteins with probe **2**, photolabelling experiments were performed with a readily available model protein, human serum albumin (HSA). Recombinant HSA (Sigma, Cat# A7736, Lot# SLBN1719V) was chosen for these experiments as ivacaftor has been reported to bind strongly to HSA *in vitro* (K_D = 15.3 ± 11.2 μM) and molecular modeling studies predicted two putative binding sites.[18] Solutions containing various concentrations and ratios of **2** and HSA were irradiated with 365 nm centered light for 30 minutes and the extent of labelling was determined by LC-MS looking for protein adducts with *m/z* indicative of covalent labelling of HSA (**Figure 2** and Supplemental Information, **Figure S2**). Two major deconvoluted mass signals were observed for unlabelled HSA, *m/z* 66321 (Peak A) and *m/z* 66440 (Peak B). Following UV irradiation of HSA in the presence of one molar equivalent of **2**, two new major peaks were observed at *m/z* 66737 (Peak C) and *m/z* 66856 (Peak D) corresponding to a shift of the two major HSA mass peaks by 416 *amu*, the mass shift predicted for monolabelling by **2**. Peaks corresponding to doubly labelled HSA (M+832) were also observed in one experiment, but to a much lesser extent and were not included in calculation of the extent of labelling. Based on the ratio of measured peak abundances of the mass-shifted signals to the residual unlabelled HSA peaks (Supplementary Information, **Table S2**) we could calculate the percentage labelling (**Figure 2**) using the general formula:

$$\%\ labelling = \frac{Peak\ A + Peak\ B}{Peak\ A + Peak\ B + Peak\ C + Peak\ D} \times 100\%$$

After 30 minutes of exposure to UV light of a 1:1 mixture of **2** and HSA (1.5 μM in 3% DMSO in water), the extent of labelled protein was determined to be 37% (**Figure 2** and Supplemental Information). Examination of the extracted ion count (EIC) after 30 min of irradiation showed a significant amount of unreacted **2** remaining (data not shown). In order to ensure that labelling was via a UV-mediated process, a 1:1 solution of HSA and probe **2** was kept in the dark and monitored by LC-MS and showed a background labelling rate of 7% after 30 min, which is significantly lower than that obtained with overt UV exposure. Competitive inhibition of the labelling of HSA by **2** with ivacaftor was evaluated to determine if the labelling events occurred in a manner specific for a putative ivacaftor binding site(s) on HSA. Addition of 150 μM ivacaftor to the solution of 1:1 mixture of **2** and HSA (both 1.5 μM in 3% DMSO in water) significantly reduced the extent of labelling by **2** (from 37% to 15%; $p < 0.0001$, **Figure 2**). No significant difference found in labelling after addition of 10 equiv (15 μM) of **1.** However, significant inhibition of labelling was observed when ivacaftor (15 μM) was first allowed to equilibrate with HSA for 30 minutes *prior* to addition of **2** and then irradiation (**Figure S3**). Photolabelling was not completely inhibited by ivacaftor under either condition indicating that at least some portion of the labelling of HSA by **2** was non-specific which is not surprizing given the micromolar binding affinity of ivacaftor for HSA (*vide supra*) (and by inference also of **2)** and the multiple potential binding sites available on HSA.

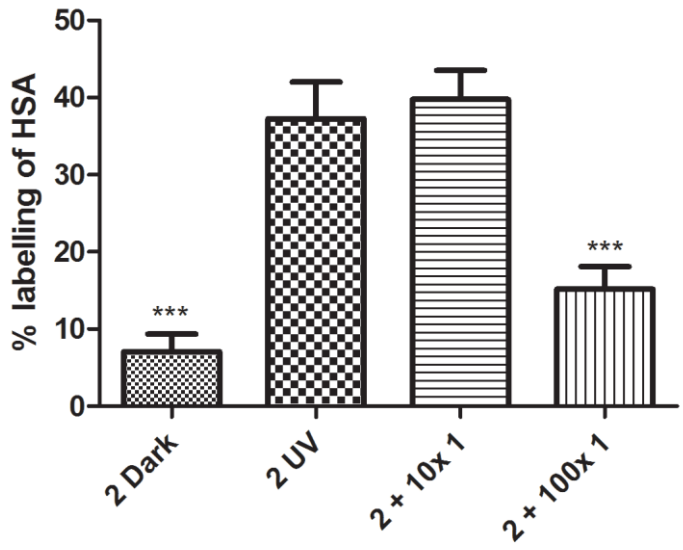

Figure 2. Photolabelling of HSA (1.5 µM in 3% DMSO in water) with **2** (1.5 µM) following 30 min of irradiation with 365 nm light, and reduction in photolabelling in presence of 10 and 100 equiv of **1** (15 µM and 150 µM respectively). Significance refers to difference from HSA + **2** + UV. *** $p<0.001$, two-tailed t-test, calculated with GraphPad Prism.

To further identify the site(s) of modification of HSA by **2**, we used tandem MS/MS and shotgun proteomics approach to identify the labelled peptides by Sequest (an automatic peptide sequencing algorithm)[20] through Discoverer 2.1 software (Thermo-Fisher Scientific). A solution of HSA, after photolabelling with **2**, was subjected to enzymatic digestion with trypsin (Trypsin Gold, Promega, Cat. No.: V5280) and the resulting peptides were analyzed on an Orbitrap Q Exactive HF (Thermo-Fisher Scientific) coupled with EASY-NLC 1000 nanoHPLC (Thermo-Fisher Scientific). In total, 7 HSA labelled peptides were identified and are tabulated in the Supplemental Information (**Table S4** and **Figures S4-S10**). The most abundantly observed labelled peptide (**P1**: [R].YTKKVPQVSTPTLVEVSR.[N], Uniprot# P02768 [437-454][21,22]) borders the known multi-drug binding site on subdomain IIIA,[22,23] that was predicted by Schneider *et al*[18] as a binding site for **1** on HSA. The location of this peptide is highlighted in red and purple on the HSA crystal structure[24] in **Figure 3**. The exact site of modification on each modified peptide was difficult to determine as the label was lost during the MS/MS fragmentation process (appearance of MH+; 417.14 Da signal, Supplemental Information **Figures S4-10**).

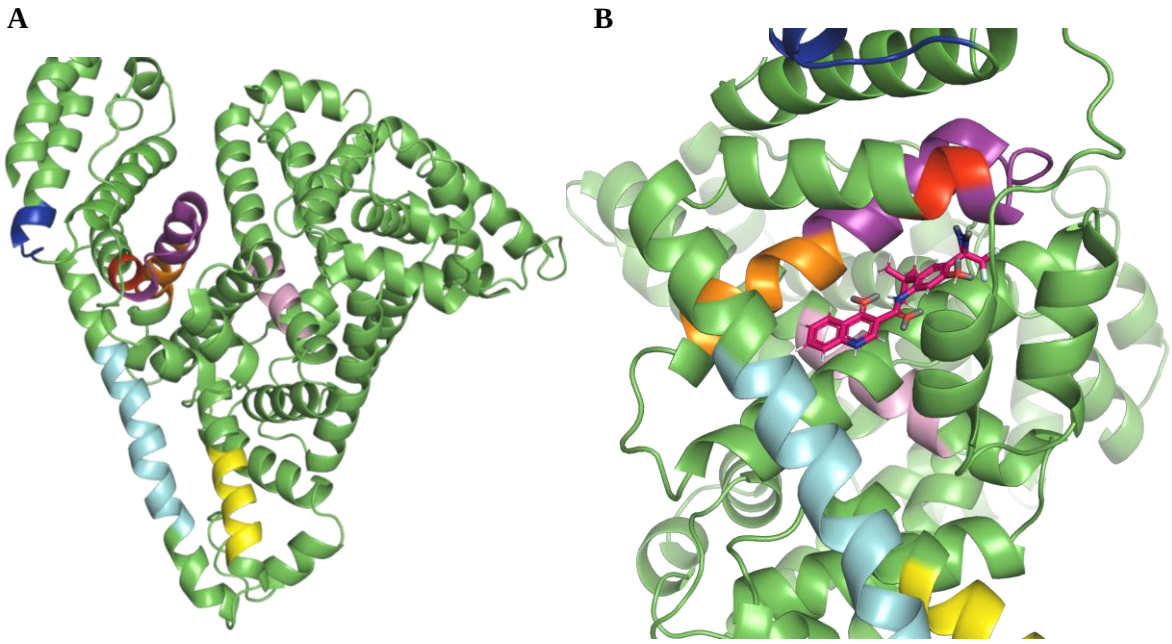

Figure 3. A) Peptides labelled by **2** identified by MS/MS on the HSA ribbon structure: **P1**, red (and purple); **P2** (overlaps with **P1**), purple; **P3**, blue; **P4**, cyan; **P5**, orange; **P6**, pink; **P7** yellow. (Graphic generated in PyMol; PDB ID: 1AO6[24]; Uniprot Assn No. P02768[21]). **B**) Probe **2** (magenta) modelled, using Genetic Optimization for Ligand Docking (GOLD) version 5.5, in the multi-drug binding site on subdomain IIIA in a manner and orientation as described for ivacaftor by Schneider *et al*[18].

In order to determine whether installation of the diazirine moiety onto the ivacaftor scaffold was deleterious to bioactivity, the ability of the probes to potentiate Wt-CFTR in HEK cells was determined using a FLIPR® membrane potential assay, where changes in fluorescence are a readout of CFTR channel activity [25,26]. A representative FLIPR® trace is shown in **Figure 4A**. The response of the CFTR channel to activation by forskolin (leading to membrane depolarization) is enhanced by the addition of ivacaftor (**1**) or probe **2**. As expected, the response to forskolin in the presence of both compounds was inhibited by the specific CFTR inhibitor: CFTRinh-172.[27] Analysis of the dose responses for each probe revealed that addition of the diazirine moiety shifted the EC_{50} for ivacaftor from 0.20 μM to 0.56 μM (**Figure 4B**) but did not significantly affect its efficacy. These results suggest that probe **2** is able to access the putative ivacaftor binding site on CFTR in a manner similar to **1.**

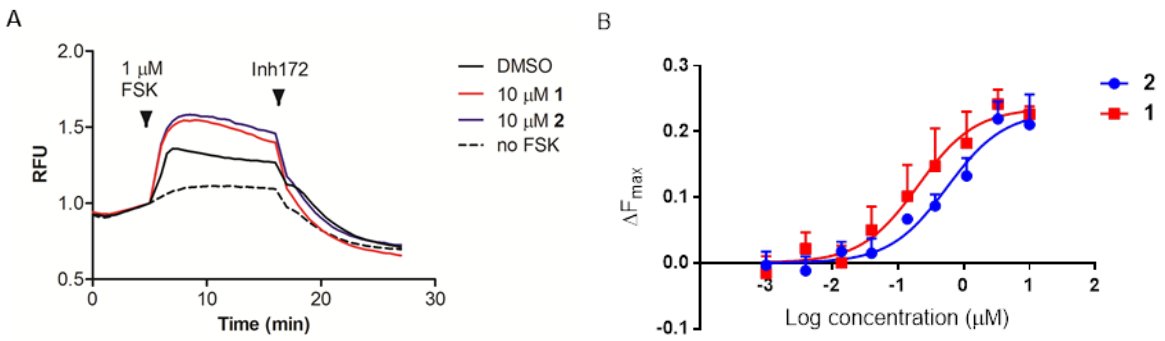

Figure 4. A) Representative trace from the FLIPR® assay comparing potentiation of Wt-CFTR in HEK cells. First arrowhead indicates the addition of 1 μM forskolin in combination with either DMSO, 10 μM ivacaftor (**1**), or 10 μM probe **2**. Second arrowhead indicates the addition of 10μM CFTR-inh172. Data was normalized to the last point of the baseline read (RFU: relative fluorescence units). B) Dose response curves of ivacaftor (**1**) and probe **2** (n=3-4). ΔF_{max} values were determined by subtracting ΔRFU_{FSK} (changes in fluorescence from forskolin addition alone) from $\Delta RFU_{FSK+probe}$ (changes in fluorescence from forskolin addition in the presence of varying concentrations of **1** or **2**). From the fitted dose response curves, the EC_{50} values of **1** and **2** were determined to be 0.20 μM and 0.56 μM, respectively.

3. Conclusions

A photoaffinity labelling probe **2,** based on the structure of ivacaftor and featuring a diazirine moiety in place of one of the *t*-butyl groups has been synthesized. The photoreactive properties of the diazirine moiety were confirmed by irradiating **2** in methanol at 365 nm to generate the methanol adduct **22**. As well, photolabelling experiments with a model protein (HSA) have shown that **2** is able to label protein efficiently and in a specific manner that can be outcompeted by ivacaftor. Potent and comparable potentiation of ion channel activity of CFTR by **2** comparable to ivacaftor has been confirmed through the use of a fluorescence-based FLIPR assay with Wt-CFTR. This probe should be useful to identify the putative binding site(s) of ivacaftor on the CFTR ion channel.

4. Experimental

4.1. General Chemistry

THF was distilled from Na and benzophenone under N_2. *N,N'*-diisopropylethylamine (DIPEA) and triethylamine (Et_3N) were distilled from CaH_2 and stored under N_2. All other reagents and solvents were

used as received from commercial suppliers unless otherwise stated. Analytical thin-layer chromatography (TLC) was performed on aluminum plates pre-coated with silica gel 60F-254 as the absorbent, and eluted with the solvent systems indicated, visualization of the plates was done with UV light (254 nm) and the indicated stains. Melting point was measured on a Fisher-Johns melting point apparatus and are uncorrected. Microwave reactions were conducted in a Biotage Initiator.

Flash chromatography was performed with a Biotage Isolera One system using SiliCycle Silia*Sep*™ Cartridges of indicated size and solvent gradient. ^{1}H, ^{19}F and ^{13}C NMR spectra were recorded with Bruker Avance II™ 600 MHz, Bruker Avance III™ 500 MHz, or Bruker Avance III™ 400 MHz. ^{1}H and ^{13}C NMR spectra were referenced to the various solvent signals[28] and processing of the spectra was performed with MestRecNova™ software (Note: numbering of atoms for the purposes of signal assignment did not follow IUPAC numbering schemes). The high-resolution mass spectra were recorded with an ESI ion source on an Agilent™ Time-of-Flight LC/MS mass spectrometer (Model 6210) using a Halo C18 (2.1x50mm) water-ACN (5mM NH_4OAc) gradient. All HPLC analyses were performed utilizing an Advanced Materials Technologies Halo™ C18 reverse-phase analytical column (4.6 × 50 mm, 5 μm) with a water-ACN (5mM NH_4OAc) gradient. All preparative HPLC purifications were carried out using a Phenomenex Kinetex C18 reverse-phase preparatory column (21.2 × 150 mm, 5 μm) with a water-ACN (5mM NH_4OAc) gradient. UV-Vis spectra were collected in solution phase in a quartz cuvette on a Varian Cary 5000 UV-Vis-NIR Spectrophotometer. ATR spectra were collected with a Perkin Elmer Spectrum Two™ FT-IR spectrometer, and absorption bands were designated as weak (w), broad (br), medium (m), or strong (s). Photo-decomposition studies were performed (when indicated) in a light-box composed of two Dreamall 36W UV Acrylic Curing Light Lamps taped together each with 4 x 9W UV bulbs emitting at 365 nm or with a UVP Mineralight© lamp (115 V, 60 Hz, 0.16 A) and irradiated at 365 nm (long UV wavelength setting).

For Single-Crystal X-ray diffraction structure determinations, single crystals were selected and mounted using Paratone oil on a 150 μm MiTeGen Dual-Thickness MicroMount. Data was collected at room temperature with a Bruker SMART APEX II Duo CCD diffractometer using a TRIUMPH graphite-

monochromated Cu-Kα radiation (λ = 1.54184 Å). Crystallographic information for **12** can be found in Supplemental Information (**Table S1**, **Figure S1**). All diffraction data were processed with the Bruker Apex II software suite. Initial solutions were obtained by using the intrinsic phasing method[29] with subsequent refinements performed with SHELXL[30] on the SHELXLE platform.[31] Diagrams were prepared by using ORTEP-3[32] and POV-RAY.[33]

4.2. 1-Bromo-5-(tert-butyl)-2-(ethoxymethoxy)-4-nitrobenzene **(5)**

To a solution of 2-bromo-4-(*tert*-butyl)-5-nitrophenol (**4**) (prepared according to DeMattei *et al*.)[19] (9.9 g, 36 mmol) in THF (60 mL) at room temperature under N_2, DIPEA (19 mL, 109 mmol) was added, followed by chloromethyl ethyl ether (5.3 mL, 58 mmol) and stirred overnight. The reaction mixture was quenched with sat. aq. NH_4Cl (100 mL), and extracted with Et_2O (50 mL, 3x). The organic layers were combined, washed with brine (100 mL), dried over Na_2SO_4, filtered, and concentrated to dryness to give compound **5** (10.7 g, 32 mmol, 89%) as a yellow crystalline solid. ^{1}H NMR (600 MHz, $CDCl_3$) δ 7.69 (s, 1H), 7.17 (s, 1H), 5.28 (s, 2H), 3.76 (q, *J* = 7.1 Hz, 2H), 1.37 (s, 9H), 1.23 (t, *J* = 7.1 Hz, 3H). ^{13}C NMR (151 MHz, $CDCl_3$) δ 152.4, 150.5, 135.8, 133.3, 115.3, 111.4, 94.3, 77.2, 65.2, 35.3, 30.8, 15.1. mp = 62 - 63 °C.

4.3. 4-Bromo-2-(tert-butyl)-5-(ethoxymethoxy)aniline **(6)**

To a solution of 1-bromo-5-(*tert*-butyl)-2-(ethoxymethoxy)-4-nitrobenzene (**5**) (502 mg, 1.51 mmol) dissolved in MeOH (15 mL), Fe powder (2 g, 36 mmol, 24 equiv), and NH_4Cl (1.5 g, 28 mmol, 18 equiv) were added and the reaction was heated at 60°C for 4 hours. The crude mixture was allowed to cool and then filtered through a bed of Celite, washed with MeOH, and the filtrate was concentrated to dryness. The crude residue was purified by automated flash chromatography on a 25 g silica cartridge (20% EtOAc/Hex isocratic elution) to give compound **6** (345 mg, 1.14 mmol, 76% yield) as a yellow oil. ^{1}H NMR ($CDCl_3$, 400 MHz) δ 7.30 (1H, s), 6.52 (1H, s), 5.22 (2H, s), 3.77 (2H, q, *J*=7.1 Hz), 1.38 (9H, s), 1.24 (3H, t, *J*=7.1 Hz). ^{13}C NMR (101 MHz, $CDCl_3$) δ 152.7, 145.1, 131.1, 129.3, 105.6, 100.7, 94.0, 77.2, 64.7, 34.0, 29.8, 15.2. HRMS: *m/z* calcd for $C_{13}H_{20}BrNO_2$: 302.0750 (M+H); found 302.0781.

4.4. tert-Butyl (4-bromo-2-(tert-butyl)-5-(ethoxymethoxy)phenyl)carbamate **(7)**

A solution of aniline **6** (2.6 g, 8.6 mmol) dissolved in toluene (5 mL) was placed in a microwave vial and then degassed under argon. Boc_2O (7.5 g, 34.4 mmol, 4 equiv) was added under argon, the microwave vial was sealed and the reaction mixture was heated in the microwave reactor for 18 h at 105 °C. The reaction mixture was cooled to room temperature and the vial was vented by puncturing the septa with a large bore needle. The crude mixture was concentrated to dryness, and the residue was purified by column chromatography on an 80 g silica cartridge (2-20 % EtOAc/Hex gradient) to give **7** (2.49 g, 6.2 mmol, 72 %) as a white crystalline solid. Remaining unreacted **6** (369 mg, 1.2 mmol, 14%) was recovered and recycled. ^{1}H NMR (500 MHz, $CDCl_3$) δ 7.48 (s, 1H), 7.46 (s, 1H), 6.35 (s, 1H), 5.28 (s, 2H), 3.79 (q, *J* = 7.1 Hz, 2H), 1.50 (s, 9H), 1.37 (s, 9H), 1.24 (t, *J* = 7.1 Hz, 3H). ^{13}C NMR (126 MHz, $CDCl_3$) δ 153.2, 152.2, 136.2, 130.9, 114.0, 108.3, 94.0, 80.8, 77.2, 64.9, 34.2, 30.8, 28.5, 15.2. HRMS: *m/z* calcd for $C_{18}H_{28}BrNO_4$: 402.1274 (M+H); found 402.1271. mp = 94 - 95 °C.

4.5. tert-Butyl (2-(tert-butyl)-5-(ethoxymethoxy)-4-(2,2,2-trifluoroacetyl)phenyl)carbamate **(8)**

A solution of **7** (526 mg, 1.31 mmol) in THF (5 mL) under N_2 was cooled to -40 °C. MeLi (1.75 mL, 2.6 mmol, 2 equiv) was added via syringe and the reaction mixture was warmed to 0 °C for 2 minutes. The reaction mixture was cooled to -78 °C and *n*-BuLi (1.30 mL, 1.96 mmol, 1.5 equiv) was added dropwise via syringe and the reaction mixture was stirred for 1 h. Ethyl trifluoroacetate (2.0 mL, 17 mmol, 13 equiv) was added quickly via syringe and the reaction mixture was warmed to room temperature. The reaction was quenched with sat. aq. NH_4Cl (10 mL), extracted into EtOAc (50 mL), then washed with brine (30 mL), dried over Na_2SO_4, filtered, and concentrated to dryness. The crude residue was purified via automated flash chromatography on a 25 g silica cartridge (2-30% EtOAc/Hex), to afford compound **8** (520 mg, 1.24 mmol, 95 % yield) as a white crystalline solid. ^{1}H NMR (400 MHz, $CDCl_3$) δ 7.97 (s, 1H), 7.72 (s, 1H), 6.88 (s, 1H), 5.32 (s, 2H), 3.77 (q, *J* = 7.1 Hz, 2H), 1.54 (s, 9H), 1.42 (s, 9H), 1.24 (t, *J* = 7.1 Hz, 3H). ^{13}C NMR (101 MHz, $CDCl_3$) δ 181.3 (q, *J* = 36.1 Hz), 157.4, 152.0, 144.0, 131.1, 130.2, 116.7

(q, *J* = 290.8 Hz), 116.4, 107.9, 93.6, 81.8, 65.1, 33.9, 30.7, 28.4, 15.1. ^{19}F NMR (376 MHz, $CDCl_3$) δ -73.68. HRMS: *m/z* calcd for $C_{20}H_{28}F_3NO_5$: 420.1992 (M+H); found 420.2003. mp = 89.5 - 90.5 ºC.

4.6. tert-butyl (2-(tert-butyl)-5-(ethoxymethoxy)-4-(2,2,2-trifluoro-1-(hydroxyimino)ethyl)phenyl)carbamate **(9)**

A solution of compound **8** (110 mg, 0.262 mmol) and hydroxylamine hydrochloride (22 mg, 0.315 mmol) in a 2:1 mixture of pyridine/MeOH (7.5 mL) was stirred at 60 ºC overnight. The reaction mixture was cooled to room temperature and concentrated to dryness. The crude residue was purified via automated flash chromatography (12 g silica cartridge, 4-40 % EtOAc/Hex gradient) to afford compound **9** (90 mg, 207 mmol, 79 % yield) as a mixture of E/Z isomers, as a white crystalline solid. ^{1}H NMR (400 MHz, $CDCl_3$) δ 8.08 (s, 1H), 7.72 (s, 1H), 7.69 (s, 1H), 7.63 (s, 2H), 7.18 (s, 2H), 7.11 (s, 1H), 6.56 (s, 2H), 5.24 (s, 4H), 5.23 (s, 2H), 3.72 (q, *J* = 7.1, 6H), 3.71 (q, *J* = 7.2 Hz, 6H),1.52 (s, 11H), 1.52 (s, 16H), 1.39 (s, 11H), 1.39 (s, 16H), 1.22 (td, *J* = 7.1, 2.1 Hz, 9H). ^{13}C NMR (151 MHz, $CDCl_3$) δ 154.8, 153.6, 147.6 (q, *J* = 32.0 Hz), 146.6 (q, *J* = 33.6 Hz), 139.1, 128.7, 127.1, 120.7 (q, *J* = 274.4 Hz), 118.2 (q, *J* = 282.3 Hz), 116.3, 112.3, 111.3, 93.5, 93.4, 81.3, 64.7, 64.6, 34.1, 34.0, 30.8, 30.7, 28.5, 15.1. ^{19}F NMR (376 MHz, $CDCl_3$) δ -65.2, -67.5. HRMS: *m/z* calcd for $C_{20}H_{29}F_3N_2O_5$: 433.1956 (M-H); found 433.2044. mp = 149 - 157 °C.

4.7. tert-butyl (2-(tert-butyl)-5-(ethoxymethoxy)-4-(2,2,2-trifluoro-1-((tosyloxy)imino)ethyl)phenyl)carbamate **(10)**

Et_3N (170 μL, 1.22 mmol, 1.5 equiv) was added to a solution of **9** (353 mg, 0.81 mmol) in DCM (10 mL) at 0 ºC, via syringe and after stirring for 5 minutes, *p*-TsCl (170 mg, 0.89 mmol, 1.1 equiv.) was added and the reaction mixture was stirred for 15 minutes while warming to room temperature. The mixture was then quenched with sat. aq. NH_4Cl (3 mL), washed with brine (3 mL), and dried (Na_2SO_4) to give tosyl oxime **10** as a crude yellow oil (495 mg) which was used directly in the subsequent step. ^{1}H NMR (400 MHz, $CDCl_3$) δ 7.9-7.85 (m, 7H), 7.76 (s, 1H), 7.69 (s, 2H), 7.38-7.35 (m, 7H), 7.02 (s, 1H), 6.90 (s, 2H), 6.61 (s, 1H), 6.60 (s, 2H), 5.15 (s, 4H), 5.13 (s, 2H), 3.63 (q, J=7.1 Hz, 4H), 3.62 (q, J=7.0 Hz, 2H), 2.48 (s,

3H), 2.46 (s, 6H), 1.53 (s, 9H), 1.51 (s, 18H), 1.38 (s, 9H), 1.34 (s, 18H), 1.19 (t, *J* = 7.1, 3H), 1.18 (t, *J* = 7.1, 6H). ^{19}F NMR (376 MHz, $CDCl_3$) δ -64.5, -67.6. HRMS: *m/z* calcd for $C_{27}H_{35}F_3N_2O_7S$: 606.2455 ($M+NH_4^+$); found 606.2508.

Alternatively, the reaction mixture could be used directly, before quenching and without workup, in the subsequent reaction to give diaziridine **11**.

4.8. tert-butyl (2-(tert-butyl)-5-(ethoxymethoxy)-4-(3-(trifluoromethyl)diaziridin-3-yl)phenyl)carbamate **(11)** *and tert-butyl (Z)-(4-((1-amino-2,2,2-trifluoroethylidene)amino)-2-(tert-butyl)-5-(ethoxymethoxy)phenyl)carbamate* **(12)**

Ammonia was condensed (~1.5 mL) at -78 °C into a sealable reaction vessel, and a portion of the reaction mixture of tosyl-oxime **10** from above (theoretical mass of 118 mg, 0.2 mmol) in DCM (3 mL) was transferred via pipette into the liquid ammonia. The reaction vessel was sealed and the reaction mixture was warmed to room temperature in a water bath and stirred overnight. The reaction vessel was cooled at -78 °C for 15 minutes then carefully opened, and the reaction mixture was warmed at room temperature for 30 minutes. The reaction mixture was concentrated to dryness and the residue was purified by column chromatography on a 25 g silica cartridge (4-40 % EtOAc/Hex) to afford a mixture of diaziridine **11** and amidine **12** in a 1:2.7 ratio by ^{1}H NMR. The mixture of diaziridine **11** and amidine **12** can then be utilized directly in the next step (oxidation to diazirine **13**) and separation of the diazirine **13** and amidine **12** post-oxidation can be performed by automated flash chromatography.

For characterization purposes a mixture of **11** and **12** (80 mg, 1:2 ratio) was separated via preparative reverse phase HPLC to give **11** as a white crystalline solid (16 mg), and **12** as a white crystalline solid (20 mg). **12** was then recrystallized from an 8:2 Et_2O/Hex mixture and the structure of **12** was confirmed by X-ray crystallography (performed by CMH with instruction and assistance from JT).

4.8.1. Characterization data for **11**

^{1}H NMR (500 MHz, $CDCl_3$) δ 7.59 (s, 1H, C-6-*H*), 7.41 (s, 1H, C-3-*H*), 6.53 (s, 1H, N-*H*), 5.35 – 5.18 (m, 2H, C-9-*H*), 3.78 – 3.70 (m, 2H, C-10-*H*), 2.65 (d, *J* = 9.0 Hz, 1H, diaziridine-N-*H*), 2.49 (d, *J* = 8.7

Hz, 1H, diaziridine-N-*H*), 1.51 (s, 9H, C-8-*H*), 1.39 (s, 9H, C-14-*H*), 1.24 (t, *J* = 7.1 Hz, 3H, C-11-*H*). ^{13}C NMR (126 MHz, $CDCl_3$) δ 154.9 (*C*-5), 153.0 (*C*-12), 138.9 (*C*-1), 133.3 (*C*-2), 128.9 (*C*-3), 123.7 (q, $^1J_{C-F}$ = 278.8 Hz, *C*-16), 115.8 (*C*-4), 110.7 (*C*-6), 93.3 (*C*-9), 81.0 (*C*-5), 64.8 (*C*-10), 56.2 (q, $^2J_{C-F}$ = 37.1 Hz, *C*-15), 34.0 (*C*-7), 30.8 (*C*-8), 28.5 (*C*-14), 15.2 (*C*-11). ^{19}F NMR (471 MHz, $CDCl_3$) δ -77.0. HRMS: *m/z* calcd for $C_{20}H_{30}F_3N_3O_4$: 472.1825 (M+K); found 472.1837. mp = 127-128 ºC.

4.8.2. Characterization data for **12.** [1]

H NMR (400 MHz, $CDCl_3$) δ 7.29 (s, 1H, C-6-*H*), 6.89 (s, 1H, C-3-*H*), 6.28 (s, 1H, N-*H*), 5.10 (s, 2H, C-9-*H*), 5.07 (s, 2H, amidine-N-*H*), 3.67 (q, *J* = 7.1 Hz, 2H, C-10-*H*), 1.48 (s, 9H, C-14-*H*), 1.34 (s, 9H, C-8-*H*), 1.18 (t, *J* = 7.1 Hz, 3H, C-11-*H*). ^{13}C NMR (101 MHz, $CDCl_3$) δ 153.9 (*C*-12), 145.3 (*C*-5), 145.3 (q, $^2J_{C-F}$ = 35.2 Hz, *C*-17), 137.7 (*C*-2), 133.0 (*C*-4), 132.7 (*C*-1), 121.3 (*C*-3), 118.3 (q, $^1J_{C-F}$ = 277.9 Hz, *C*-18), 116.6 (*C*-6), 94.5 (*C*-9), 80.4 (*C*-13), 64.6 (*C*-10), 34.3 (*C*-7), 30.8 (*C*-8), 28.5 (*C*-14), 15.0 (*C*-11). ^{19}F NMR (376 MHz, $CDCl_3$) δ -72.80. HRMS: *m/z* calcd for $C_{20}H_{30}F_3N_3O_4$: 434.2261 (M+H); found 434.2249. mp = 124 - 126 °C. IR (cm^{-1}) 3427 (w), 3288 (w), 3186 (w), 2981-2896 (m), 1700 (s), 1682 (s), 1625 (w), 1483 (s),1139 (s).

4.9. tert-Butyl (2-(tert-butyl)-5-(ethoxymethoxy)-4-(3-(trifluoromethyl)-3H-diazirin-3-yl)phenyl)carbamate **(13)**

The mixture from above containing diaziridine **11** and amidine **12** (222 mg, **11**:**12** in ratio of 1:1.6, total 0.5 mmol) **(**calculated **11**, 0.2 mmol) was dissolved in MeOH (3 mL) and Et_3N (180 µl, 1.28 mmol, 2.5 equiv) was added and the reaction mixture was stirred for 5 minutes. I_2 (71 mg, 0.56 mmol, 1.1 equiv) was added and the reaction mixture was stirred overnight and monitored by TLC. The reaction mixture was quenched with $Na_2S_2O_3$ (aq.) and extracted into EtOAc (30 mL). The organic fractions were combined and washed with sat. aq. $NaHCO_3$ (10 mL), brine (10 mL), dried over Na_2SO_4, and concentrated to dryness. The crude residue was purified by automated flash chromatography on a 12 g silica cartridge (4-40% EtOAc/Hex gradient) to give compound **13** (63 mg, 0.15 mmol, 18% yield over 3 steps) as a white

crystalline solid. ^{1}H NMR (400 MHz, CD_3OD) δ 7.46 (s, 1H, C-3-*H*), 7.16 (s, 1H, C-6-*H*), 5.34 (s, 2H, C-9-*H*), 3.78 (q, *J* = 7.1 Hz, 2H, C-10-*H*), 1.50 (s, 9H, C-14-*H*), 1.37 (s, 9H, C-8-*H*), 1.22 (t, *J* = 7.1 Hz, 3H, C-11-*H*). ^{13}C NMR (151 MHz, CD_3OD) δ 157.3 (*C*-5), 156.6 (*C*-12), 140.9 (*C*-2), 140.7 (*C*-4), 129.7 (*C*-3), 123.6 (q, $^{1}J_{C\text{-}F}$ = 273.9 Hz, *C*-16), 117.8 (*C*-6), 115.6 (*C*-1), 94.4 (*C*-9), 81.5 (*C*-13), 65.7 (*C*-10), 35.5 (*C*-7), 31.1 (*C*-8), 28.7 (*C*-14), 27.6 (q, $^{2}J_{C\text{-}F}$ = 42.4 Hz, *C*-15), 15.4 (*C*-11). ^{19}F NMR (376 MHz, CD_3OD) δ -70.7. HRMS: *m/z* calcd for $C_{20}H_{28}F_3N_3O_4$: 449.2370 ($M+NH_4^+$); found 449.2365.

4.10. tert-Butyl (2-(tert-butyl)-5-(ethoxymethoxy)-4-(2,2,2-trifluoro-1-methoxyethyl)phenyl)carbamate **(15)**

A solution of diazirine **13** (3 mg, 7 μmol) dissolved in MeOH (300 μL) was placed in an NMR tube, which was suspended in a UV light-box comprised of two Dreamall UV lamps (described above) and irradiated for 48h. The reaction mixture was concentrated to dryness to give the methanol adduct **15** as a white solid (3 mg, 6.9 μmol, quantitative yield). ^{1}H NMR (600 MHz, MeOD) δ 7.50 (s, 1H), 7.10 (s, 1H), 5.29 – 5.23 (m, 2H), 5.14 (q, $^{3}J_{H\text{-}F}$ = 6.7 Hz, 1H), 3.72 (q, *J* = 7.1 Hz, 2H), 3.35 (s, 3H), 1.51 (s, 9H), 1.38 (s, 9H), 1.21 (t, *J* = 7.1 Hz, 3H). ^{13}C NMR (151 MHz, MeOD) δ 157.0, 155.7, 140.8, 138.7, 127.5, 125.5 (q, $^{1}J_{C\text{-}F}$= 281.2 Hz), 120.4, 117.5, 94.5, 81.2, 75.3 (q, $^{2}J_{C\text{-}F}$ = 31.9 Hz), 65.5, 58.3, 35.6, 31.3, 28.8, 15.4. ^{19}F NMR (376 MHz, CD_3OD) δ -78.2. HRMS: *m/z* calcd for $C_{21}H_{32}F_3NO_5$: 453.2571 $[M+NH_4]^+$; found 453.2577. mp = 71 – 73 °C

4.11. 5-Amino-4-(tert-butyl)-2-(3-(trifluoromethyl)-3H-diazirin-3-yl)phenol **(3)**

To a solution of compound **13** (62 mg, 0.144 mmol) dissolved in MeOH (1 mL), sat. methanolic HCl (1 mL, prepared by bubbling HCl (*g*) through methanol) was added and the reaction mixture was stirred for 1 hour, monitored by TLC and LC-MS. The reaction mixture was blown dry under a stream of nitrogen to give compound **3** (34 mg, 0.124 mmol, 86 % yield) as the HCl salt as a crystalline solid which was used immediately in subsequent reactions. ^{1}H NMR (500 MHz, CD_3OD) δ 7.29 (s, 1H), 6.44 (s, 1H), 1.38 (s, 9H). ^{19}F NMR (471 MHz, CD_3OD) δ -70.68. HRMS: *m/z* calcd for $C_{12}H_{14}F_3N_3O$: 274.1162 (M+H); found 274.1142.

4.12. N-(4-bromo-2-(tert-butyl)-5-(ethoxymethoxy)phenyl)-4-oxo-1,4-dihydroquinoline-3-carboxamide **(16)**

A mixture of aniline **6** (2.00 g, 6.62 mmol), HATU (5.03 g, 6.62 mmol, 2 equiv), 1,4-dihydro-4-oxoquinoline-3-carboxylic acid (**14**) (1.88 g, 9.93 mmol, 1.5 equiv), DMAP (81 mg, 0.66 mmol, 0.1 equiv), and HOBt (895 mg, 6.62 mmol, 1 equiv) were dissolved in DMF (20 mL). DIPEA (3.5 mL, 19.9 mmol, 3 equiv.) was added and the reaction mixture was stirred overnight at 60 °C. The reaction mixture was cooled to room temperature and concentrated to remove DMF. The crude residue was diluted with EtOAc (200 mL) and washed with sat. aq. $NaHCO_3$ (100 mL), brine (50 mL), dried over Na_2SO_4, and concentrated to dryness. The crude residue was purified by automated flash chromatography on an 80 g silica cartridge (75-100% EtOAc/Hex) to give amide **16** as a white crystalline solid (2.6 g, 5.5 mmol, 83 % yield). ^{1}H NMR (500 MHz, $CDCl_3$) δ 12.60 (s, 1H), 12.52 (d, *J* = 6.4 Hz, 1H), 9.08 (d, *J* = 6.8 Hz, 1H), 8.43 (dd, *J* = 1.8, 7.8 Hz, 1H), 7.77 (s, 1H), 7.48 – 7.40 (m, 2H), 7.34 (s, 1H), 6.02 (dd, *J* = 1.2, 7.4 Hz, 1H), 5.08 (s, 2H), 3.48 (q, *J* = 7.1 Hz, 2H), 1.45 (s, 9H), 0.97 (t, *J* = 7.1 Hz, 3H). ^{13}C NMR (126 MHz, $CDCl_3$) δ 177.9, 165.8, 152.5, 144.4, 141.4, 139.2, 135.5, 133.1, 131.7, 126.6, 126.1, 125.6, 118.6, 117.9, 111.0, 110.3, 93.8, 77.2, 64.8, 34.8, 30.8, 14.9. HRMS: *m/z* calcd for $C_{23}H_{25}BrN_2O_4$: 473.1071 (M+H); found 473.1051. mp = 205 - 206.5 °C.

4.13. N-(2-(tert-butyl)-5-(ethoxymethoxy)-4-(2,2,2-trifluoroacetyl)phenyl)-4-oxo-1,4-dihydroquinoline-3-carboxamide **(17)**

A solution of compound **16** (230 mg, 0.486 mmol) in THF (10 mL) under N_2 was cooled at -40 °C and MeLi (1.6 M, 700 μL, 1.12 mmol, 2.3 equiv) was added via syringe and the reaction mixture was stirred for 2 min. At -40 °C, *n*-BuLi (1.58 M, 370 μL, 0.583 mmol, 1.5 equiv) was added dropwise via syringe and the reaction mixture was stirred a further 15 minutes. Ethyl trifluoroacetate (1.7 mL, 15 mmol, 30 equiv) was added quickly via syringe and the reaction mixture was warmed to 0 °C then quenched with saturated aqueous NH_4Cl (1 mL). The reaction mixture was extracted into EtOAc (5 mL) and the organic fractions were combined and washed with brine (2 mL) dried over Na_2SO_4 and concentrated to dryness to give

crude compound **17** as a yellow oil (270 mg). This crude material was utilized without purification in the subsequent oxime formation reaction.

For characterization purposes a portion of crude residue was purified by preparative reverse phase HPLC then lyophilized to give **17** (11 mg, 0.022 mmol, 53% yield from 0.042 mmol of **16**) as a white crystalline solid. The chromatogram from preparative HPLC at 254 nm showed conversion to **17** of approximately 65 % and based on this value the product was approximately 0.32 mmol in the crude mixture.

^{1}H NMR (600 MHz, $CDCl_3$) δ 12.66 (s, 1H), 11.63 (s, 1H), 9.01 (s, 1H), 8.49 – 8.42 (m, 1H), 7.91 (s, 1H), 7.78 (s, 1H,), 7.44 (m, 2H), 6.65 (d, *J* = 7.4 Hz, 1H), 5.19 (s, 2H), 3.59 (q, *J* = 7.1 Hz, 2H), 1.52 (s, 9H), 1.08 (t, *J* = 7.1 Hz, 3H). ^{13}C NMR (151 MHz, $CDCl_3$) δ 182.4 (q, $^{2}J_{C\text{-}F}$ = 36.0 Hz), 177.7, 165.2, 156.2, 144.4, 142.8, 139.0, 137.9, 133.2, 130.4, 126.7, 126.6, 125.9, 119.4, 118.2, 116.5 (q, $^{1}J_{C\text{-}F}$ = 290.7 Hz), 114.8, 110.7, 93.4, 65.2, 34.8, 30.5, 15.0. HRMS: *m/z* calcd for $C_{25}H_{26}F_3N_2O_5$: 491.1788 (M+H); found 491.1741 *m/z*. mp = 107 – 109 °C.

4.14. N-(2-(tert-butyl)-5-(ethoxymethoxy)-4-(2,2,2-trifluoro-1-(hydroxyimino)ethyl)phenyl)-4-oxo-1,4-dihydroquinoline-3-carboxamide **(18)**

Hydroxylamine hydrochloride (42 mg, 0.61 mmol, ~1.9 equiv) was added to the crude residue containing compound **17** obtained in the previous reaction (270 mg, ~0.32 mmol) in a 2:1 mixture of pyridine/MeOH, and the reaction mixture was heated overnight at 60 °C. The crude reaction mixture was cooled to room temperature, concentrated to dryness, and the residue was purified by automated flash chromatography on a 12 g silica column (30-100% EtOAc/Hex gradient). The purified product was recrystallized from a 1:10:2 MeOH/DCM/Hexanes mixture to give compound **18** (285 mg, 0.56 mmol, 53% yield over two steps) as a white solid (>95% pure by HPLC). ^{1}H NMR (400 MHz, CD_3OD) δ 8.90 (s, 1H), 8.43 (dd, *J* = 1.4, 8.3 Hz, 1H), 7.82 (ddd, *J* = 1.5, 7.1, 8.5 Hz, 1H), 7.67 (d, *J* = 8.3 Hz, 1H), 7.60 – 7.51 (m, 3H), 7.31 (s, 1H), 7.22 (s, 1H), 5.26 (s, 2H), 5.24 (s, 2H), 3.72 (q, *J* = 7.1 Hz, 2H), 3.72 (q, *J* = 7.1 Hz, 2H), 1.48 (s, 9H), 1.47 (s, 9H), 1.20 (t, *J* = 7.1 Hz, 3H), 1.19 (t, *J* = 7.1 Hz, 3H). ^{13}C NMR (101 MHz, CD_3OD) δ 178.8, 166.1, 166.0, 155.7, 154.5, 146.6, 145.7, 140.8, 138.9, 138.7, 138.2, 138.2, 134.4, 130.0, 128.5, 127.7,

127.0, 126.8, 124.0, 122.5, 121.2, 120.0, 120.0, 118.4, 116.4, 116.1, 116.1, 115.8, 115.8, 112.0, 101.4, 94.7, 94.4, 65.5, 49.0, 35.2, 31.0, 15.4. ^{19}F NMR (376 MHz, CD_3OD) δ -66.5, -68.5..HRMS: *m/z* calcd for $C_{25}H_{26}F_3N_3O_5$: 506.1897 (M+H); found 506.1920. mp = 207 - 210 °C.

4.15. N-(2-(tert-butyl)-5-(ethoxymethoxy)-4-(3-(trifluoromethyl)diaziridin-3-yl)phenyl)-4-oxo-1,4-dihydroquinoline-3-carboxamide **(19)** *and (Z)-N-(4-((1-amino-2,2,2-trifluoroethylidene)amino)-2-(tert-butyl)-5-hydroxyphenyl)-4-oxo-1,4-dihydroquinoline-3-carboxamide* **(20)**

DIPEA (133 µL, 0.75 mmol, 3 equiv) was added to a solution of oxime **18** (126 mg, 0.250 mmol) in DCM, and stirred until all solids dissolved; then the reaction mixture was cooled to 0 °C and *p*-TsCl (62 mg, 1.3 equiv) was added. The reaction mixture was stirred for 15 minutes, then warmed to room temperature, and stirred for 15 minutes. The progress of the reaction was monitored by LC-MS. The crude reaction mixture was added directly to a sealable vessel containing NH_3 (*l*) at -40 °C. The reaction mixture was sealed in the vessel and stirred overnight at room temperature. The reaction mixture was cooled to -60 °C and stirred for 15 minutes, then the reaction vessel was opened, and the reaction mixture was allowed to warm to room temperature and stirred for 15 minutes. The reaction mixture was purified by preparative-scale HPLC, (55% ACN/H_2O, 5mM NH_4OAc isocratic elution) and lyophilized to give diaziridine **19** (44 mg, 0.087 mmol, 35% over 2 steps), and amidine **20** (20 mg, 0.040 mmol, 13 % from **18**) as white amorphous solids.

4.15.1. Characterization data for **19**

^{1}H NMR (601 MHz, $CDCl_3$) δ 12.51 (s, 1H), 11.97 (s, 1H), 9.05 (d, *J* = 4.5 Hz, 1H), 8.45 (dd, *J* = 1.5, 8.1 Hz, 1H), 7.70 (s, 1H), 7.51 – 7.45 (m, 2H), 7.44 – 7.39 (m, 1H), 6.35 (d, *J* = 8.2 Hz, 1H), 5.11 (s, 2H), 3.59 – 3.45 (m, 2H), 2.72 (d, *J* = 9.0 Hz, 1H, diaziridine-N-*H*), 2.32 (d, *J* = 9.0 Hz, 1H, diaziridine-N-*H*), 1.50 (s, 9H), 1.04 (t, *J* = 7.1 Hz, 3H). ^{13}C NMR (151 MHz, $CDCl_3$) δ 177.7, 165.4, 154.6, 144.4, 139.1, 138.5, 138.1, 132.9, 129.7, 126.7, 126.5, 125.6, 123.6 (q, $^1J_{C\text{-}F}$ = 279.1 Hz), 118.3, 118.3, 115.1, 110.7, 93.1, 64.8, 56.3 (q, $^2J_{C\text{-}F}$ = 37.0 Hz), 34.7, 30.8, 15.0. ^{19}F NMR (471 MHz, $CDCl_3$) δ -76.86. HRMS: *m/z* calcd for

$C_{25}H_{27}F_3N_4O_4$: 505.2057 (M+H); found 505.2085. mp = 145 - 147 °C. IR (cm^{-1}): 3235 (w), 2959 (w), 1644 (m), 1568 (m), 1520 (s), 1476 (s), 1148 (s).

4.15.2. Characterization data for **20.**

^{1}H NMR (400 MHz, Acetone-d_6) δ 11.94 (s, 1H), 8.96 (s, 1H), 8.44 (ddd, *J* = 0.7, 1.4, 8.1 Hz, 1H), 7.95 – 7.71 (m, 2H), 7.60 (s, 1H), 7.54 (ddd, *J* = 1.7, 6.4, 8.2 Hz, 1H), 6.91 (s, 1H), 6.47 (s, 2H), 5.16 (s, 2H), 3.72 (q, *J* = 7.1 Hz, 2H), 1.46 (s, 9H), 1.16 (t, *J* = 7.1 Hz, 3H). ^{13}C NMR (151 MHz, Acetone-d_6) δ 177.0, 177.0, 163.0, 162.9, 145.5, 145.4 (q, *J* = 34.1 Hz), 145.3 (q, *J* = 34.2 Hz), 144.1, 139.4, 137.2, 137.2, 133.8, 132.8, 132.2, 132.1, 126.7, 126.7, 126.0, 125.0, 125.0, 120.2, 118.9 (q, *J* = 278.6 Hz), 118.8, 117.1, 117.0, 111.9, 111.9, 93.9, 63.9, 34.0, 30.0, 30.0, 14.5. ^{19}F NMR (376 MHz, Acetone-d_6) δ -73.1, -73.1. HRMS: *m/z* calcd for $C_{25}H_{27}F_3N_4O_4$: 505.2057 (M+H); found 505.1870.

4.16. N-(2-(tert-butyl)-5-(ethoxymethoxy)-4-(3-(trifluoromethyl)-3H-diazirin-3-yl)phenyl)-4-oxo-1,4-dihydroquinoline-3-carboxamide **(21)**

DMP (38 mg, 0.090 mmol, 3.0 equiv.) was added to a solution of diaziridine **19** (15 mg, 0.030 mmol) in DCM (300 μL) in an amber vial wrapped in foil and the reaction mixture was stirred for 1 hour. The reaction mixture was quenched with 1M aqueous NaOH (2 mL), and the organic layer was washed with H_2O (2 mL), brine (1 mL) and dried over Na_2SO_4, filtered, and blown dry under a stream of N_2 then dried under vacuum to give **21** (11 mg, 0.022 mmol, 74% yield) as a white powder (>95% pure by ^{1}H NMR and LC-MS). ^{1}H NMR (600 MHz, $CDCl_3$) δ 12.57 (s, 1H), 12.08 (s, 1H), 9.04 (d, *J* = 4.9 Hz, 1H), 8.44 (dd, *J* = 1.5, 8.1 Hz, 1H), 7.64 (s, 1H), 7.48 (s, 1H), 7.42 (ddd, *J* = 1.1, 7.0, 8.1 Hz, 1H), 7.30 – 7.25 (m, 1H), 6.30 (d, *J* = 8.3 Hz, 1H), 5.15 (s, 2H), 3.56 (q, *J* = 7.1 Hz, 2H), 1.48 (s, 9H), 1.03 (t, *J* = 7.1 Hz, 3H). ^{13}C NMR (151 MHz, $CDCl_3$) δ 177.7, 165.5, 155.9, 144.3, 139.2, 139.1, 138.8, 133.0, 129.2, 126.6, 126.4, 125.6, 122.2 (q, $^1J_{C\text{-}F}$ = 274.9 Hz), 118.1, 115.6, 115.0, 110.5, 93.0, 64.8, 34.7, 30.7, 26.6 (q, $^2J_{C\text{-}F}$ = 42.6 Hz), 15.0. ^{19}F NMR (376 MHz, $CDCl_3$) δ -68.7. HRMS: *m/z* calcd for $C_{25}H_{25}F_3N_4O_4$: 503.1901 (M+H); found 503.1914.

4.17. N-(2-(tert-butyl)-5-hydroxy-4-(3-(trifluoromethyl)-3H-diazirin-3-yl)phenyl)-4-oxo-1,4-dihydroquinoline-3-carboxamide **(2)**

Saturated methanolic HCl (250 μL) was added to a solution of diazirine **21** (11 mg, 0.022 mmol) in MeOH (400 μL), in an amber vial wrapped in foil and the reaction mixture was stirred at room temperature for 2 hours. The progress of the reaction was monitored by LC-MS and TLC (EtOAc). The reaction mixture was blown dry under a stream of N_2 (*g*) and then placed under high vacuum to give phenol **2** (10 mg, 0.022 mmol, quant. yield) as a white solid residue. ^{1}H NMR (600 MHz, CD_3OD) δ 8.88 (s, 1H, C-*H*-19), 8.41 (d, J = 8.0 Hz, 1H, C-*H*-23), 7.82 (t, J = 7.5 Hz, 1H, C-*H*-25), 7.68 (d, J = 8.1 Hz, 1H, C-*H*-26), 7.56 (t, J = 7.4 Hz, 1H, C-*H*-24), 7.44 (s, 1H, C-*H*-3), 7.23 (s, 1H, C-*H*-6), 1.45 (s, 9H, C-*H*-8). ^{13}C NMR (151 MHz, CD_3OD) δ 178.7 (*C*-21), 165.8 (*C*-28), 157.7 (*C*-5), 145.6 (*C*-19), 140.7 (*C*- 27), 139.4 (*C*-1), 136.5 (*C*-2), 134.5 (*C*-25), 129.4 (*C*-3), 127.6 (*C*-22), 126.9 (*C*-23), 126.8 (*C*-24), 123.8 (q, J = 273.9 Hz, *C*-16), 120.0 (*C*-26), 117.1 (*C*-6), 112.5 (*C*-4), 111.8 (*C*-23), 35.1 (*C*-7), 30.9 (*C*-8), 27.6 (q, J = 42.5 Hz, *C*-15). ^{19}F NMR (376 MHz, CD_3OD) δ -70.54. HRMS: *m/z* calcd for $C_{22}H_{19}F_3N_4O_3$: 445.1487 (M+H); found 445.1474. UV (MeOH) λ_{max} 311 nm.

4.18. N-(2-(tert-butyl)-5-hydroxy-4-(2,2,2-trifluoro-1-methoxyethyl)phenyl)-4-oxo-1,4-dihydroquinoline-3-carboxamide **(22)**

A solution of diazirine **2** (7 mg, 0.016 mmol) in MeOH (1 mL), in a clear vial was placed on its side onto an upturned UVP Mineralight© lamp (115 V, 60 Hz, 0.16 A) and irradiated at 365 nm (long UV wavelength setting). The progress of the reaction was monitored by HPLC and LC-MS. After 3 hours of irradiation the majority of the starting material was converted to a new species with mass corresponding to the methanol adduct, the reaction mixture was then blown dry under nitrogen. A pure sample of **22** was obtained by silica chromatography (75-100 % EtOAc/Hex); compound **22** (1 mg). ^{1}H NMR (400 MHz, CD_3OD) δ 8.90 (s, 1H), 8.43 (dd, *J* = 1.2, 8.1 Hz, 1H), 7.82 (ddd, *J* = 1.5, 7.0, 8.4 Hz, 1H), 7.68 (d, *J* = 8.0 Hz, 1H), 7.56 (ddd, *J* = 1.1, 7.0, 8.2 Hz, 1H), 7.49 (s, 1H), 7.13 (s, 1H), 5.16 (q, *J* = 6.9 Hz, 1H), 3.38 (s, 3H), 1.45 (s, 9H). ^{13}C NMR (151 MHz, CD_3OD) δ 178.8, 166.0, 155.8, 145.6, 140.8, 137.6, 136.6, 134.4,

127.7, 127.3, 126.9, 126.8, 125.8 (q, *J* = 280.2, 280.7 Hz), 120.0, 117.5, 116.7, 112.1, 75.4 (q, *J* = 31.4 Hz), 58.1, 35.2, 31.2. ^{19}F NMR (376 MHz, CD_3OD) δ -78.1. HRMS: *m/z* calcd for $C_{23}H_{23}F_3N_2O_4$: 449.1683 (M+H); found 449.1683.

4.19. FLiPR membrane potential assay:

The FLiPR membrane potential assay was conducted as previously described by Molinski *et al.*[34]
HEK cells expressing Wt-CFTR were grown in black 96 well Costar plates with clear bottoms at 37°C with 5% CO_2. When the cells reached 100% confluency, they were loaded with blue membrane potential dye (Molecular Probes™) at 0.5 mg/mL dissolved in a buffer containing 136 mM sodium gluconate, 3 mM potassium gluconate, 10 mM glucose and 20 mM HEPES (pH 7.35, 300mOsm). After a 45 minute incubation time at 37 °C, the plate fluorescence was read with a SpectraMax i3x plate reader (Molecular Devices) with the excitation and emission wavelengths set at 530nm and 560nm, respectively.
The baseline was first read for five minutes. Forskolin (Sigma), VX-770 or its analog were added subsequently to stimulate CFTR channel activity for 10 minutes; CFTR inhibitor 172 (Cystic Fibrosis Foundation Therapeutics) was added at the end of the assay to inhibit CFTR channel activity for 10 minutes.
Statistical analysis was performed using GraphPad Prism v6.01.

4.20. Photolabelling of HSA:

Lyophilized recombinant human serum albumin (HSA) (Lot # SLBN1719V) was purchased from Sigma-Aldrich. A stock solution of 30 µM HSA was prepared by dissolving 2 mg HSA in 1mL of milliQ deionized water, and then filtering through a 0.45 µm syringe filter. A 2.25 mM in DMSO stock solution of probe **2** was prepared by dissolving 1 mg of **2** in 1 mL of DMSO and was stored at -20 °C wrapped in foil. Similarly, 2.25 mM and 22.5 mM stock solutions of ivacaftor were also prepared in DMSO. Solutions of 1.5 µM HSA, 1.5 µM **2**, and 0, 10, and 100 uM ivacaftor (**1**) in 3% DMSO in 1 mL water were prepared in HPLC vials. Each solution was prepared by adding the stock probe **2** solution and varying amounts of

the stock ivacaftor solutions to a clear conical HPLC vial, diluting the mixture up to 30 µL in DMSO and then adding 920 µL of milliQ water before sealing the vials. 50 µL of HSA stock solution was then added through the septa via syringe and the solution was vortexed for 5 seconds. The samples were then analyzed by LC-MS to obtain zero time reading. Following t = 0 time-point, each vial (except for dark controls which were kept wrapped in foil) was placed on a UVP Mineralight© lamp (115 V, 60 Hz, 0.16 A) and irradiated at 365 nm (long UV wavelength setting) for 30 minutes and then analyzed by LC-MS. Deconvolution of the TIC signal was performed in MassHunter™ to obtain the mass spectrum for HSA. The peak lists for each HSA mass spectrum time point were exported to a spreadsheet (Supplemental Information **Table S2**). The percent labelling value was calculated from the ratio of peak abundances of the major labelled and unlabelled HSA peaks at t = 30 min using the following formula (**Section 2.3**):

$$\%\ labelling = \frac{Peak\ A + Peak\ B}{Peak\ A + Peak\ B + Peak\ C + Peak\ D} \times 100\%$$

4.21. Trypsin digestion of labelled HSA and proteomics analysis:

A 1 mL 3% DMSO solution of **2** (1.5 nmol) and lyophilized human serum albumin (HSA, 1.5 nmol) was prepared and irradiated as above for 30 minutes and then concentrated to dryness on a Thermo Scientific Savant SpeedVac® Concentrator (SPD131DDA) before being reconstituted in 36.5 µL 40 mM Tris at pH 8.0, 10 µL 50 mM EDTA, 10 µL 0.1 M TCEP, 2.5 µL 20% SDS, and heated at 100 °C for 10 min. Urea powder of 48 mg was then added and the solution was incubated at 37 °C for 30 min with agitation on a shaker plate. Subsequently, 1.4 µL 0.5 M iodoacetamide (IAA) was introduced and the solution was incubated in the dark for 30 min at room temperature. Excessive IAA was quenched by 2.8 µL 1 M dithiothreitol (DTT) at room temperature for 15 min. The sample solution was diluted to 1 mL with 20 mM Tris at pH 8.0 prior to the addition of 5 µg of trypsin (Trypsin gold, Promega, Cat. No. V5280) to affect proteolysis at 37 °C for 16 h with agitation on a shaker plate. The digested peptide solution was then acidified to pH ~ 3 with 1 M HCl and loaded onto an Oasis ® MCX 1cc cartridge (Waters Co., Lot No. 013037086A) for desalting. The eluted peptides were dried on the SpeedVac®.

4.21.1. Mass Spectrometry analysis of HSA peptide fragments:

The purified peptides were dissolved in 40 µL of 0.1% formic acid and analyzed on a Q Exactive HF Orbitrap® mass spectrometer (Thermo Scientific, Mississauga, ON, Canada) coupled with an EASY nLC 1000® (Thermo Scientific) UHPLC through the nano-EASY spray source (Thermo Scientific) for the analyses. The separation was carried out using commercial Pepmap EASY-spray® C18 trap and analytical columns (Thermo Fisher) of 75 µm ID, 3 µm C18 resin with 100 Å pore size at 20 and 150 mm length respectively for a 20 min gradient of 2−35% buffer B (0.1% FA in acetonitrile), as detailed previously (Sun et al. JPR, 2017).[35] A voltage of 2.0 kV was used for electrospray, and the ion transfer tube that guided ions from spray into MS had a temperature of 250 ℃.

For Q-Exactive HF MS/MS analysis, data-dependent method was used to select top 5 most abundant precursor ions in MS 1 scan for high collision dissociation (HCD) MS/MS fragmentation with a dynamic exclusion of 10 sec. The MS1 precursor scan was acquired at m/z range of 400-2000 with mass resolution of 60,000 and the MS2 resolution is 15, 000. The automatic gain control (AGC) value for MS1 and MS2 scans is of 1E6 and 1E3, respectively. Precursors with changes of >5, and the unassigned were excluded from MS2 scans.

*4.21.2. MS/MS data analysis***:**

The resolved raw files from Q-Exactive HF® were processed by Proteome Discoverer 2.1® (Thermo Scientific, Mississauga, ON, Canada) and searched using Sequest HT®. The acquired spectra were searched against a customized database, combining target HSA sequence with the yeast Uniprot database and common contaminants.[35] The monoisotopic precursor mass tolerance was 10 ppm, and the monoisotopoic fragment mass tolerance was 0.02Da. Criteria of a minimum of 6 amino acids and 2 miss cleavages were used for search. Cysteine carbamidomethylation (+57.05130) was treated as a fixed modification, and all the other amino acids were treated as the dynamic modification (+416.13478) by the insertion of carbene species generated from probe **2**. The reversed sequences of the original searching

database were used as the decoy database for FDR estimation. The strict FDR cutoff: 0.01 and Percolator were used to filter the false positives. All the HSA peptides identified with labelling (Supplemental Information: **Table S4**, **Figures S4-S10**) were further manual verified for accuracy.

Conflict of Interest Disclosure

The authors declare no competing financial interest.

Author information

Corresponding Author

*Tel: +1(778) 782-3351. Fax: +1(778) 782-3765. E-mail: robert_young@sfu.ca.

ORCID

Robert N. Young: 0000-0002-8235-6080

Christine E. Bear: 0000-0001-7063-3418

Author contributions

C.M.H developed the design of the syntheses, synthesized all of the compounds reported in the manuscript, carried out the photolysis and trypsin degradation assays, prepared schemes, wrote the body of the narrative and experimental section, and edited the manuscript. M.H. performed the biological assays. G.C. provided technical/analytical support, synthetic expertise, and edited the manuscript. Z.Q. established protocols for analyzing HSA by LC-MS which were utilized by C.M.H. B.S oversaw the proteolysis and MS/MS studies and performed the MS/MS analysis. C.B. oversaw the biological testing. R.N.Y. conceptualized the project, designed the probes and general approaches for their synthesis, analyzed and interpreted data and edited the manuscript**.**

Acknowledgements

The authors acknowledge the financial support of Cystic Fibrosis Canada (Grant #3224) at both Simon Fraser University and The Hospital for Sick Children Sites. Grant funding from CIHR: MOP097954, as well as financial support from Simon Fraser University.

Abbreviations

CF, cystic fibrosis; CFTR, cystic fibrosis transmembrane conductance regulator protein; DTT, dithiothreitol; EIC, extracted ion signal; Et_3N, trimethylamine; FLIPR, fluorescent imaging plate reader; FSK, forskolin; DIPEA, *N*,*N*-diisopropylethyl amine; HATU, 1-[Bis(dimethylamino)methylene]-1H-1,2,3-triazolo[4,5-b]pyridinium-3-oxide hexafluorophosphate; HOBt, hydroxybenzotriazole; IAA, iodoacetamide; PAL, photoaffinity ligand.

Supplementary Information

The following is the supplementary data related to this article: NMR characterization data for all novel compounds synthesized, data for MS analysis of HSA photolabelling and proteomics, and crystallographic information and data in CIF format CCDC 1822252.

References

(1) Cant, N.; Pollock, N.; Ford, R. C. *Int. J. Biochem. Cell Biol.* **2014**, *52*, 15–25.

(2) Stephenson, A.; Beauchamp, N. *The Canadian Cystic Fibrosis Registry: 2013 Annual Report*; 2013.

(3) Rommens, J.; Iannuzzi, M.; Kerem, B.; Drumm, M.; Melmer, G.; Dean, M.; Rozmahel, R.; Cole, J.; Kennedy, D.; Hidaka, N.; Et, A. *Science.* **1989**, *245* (4922), 1059–1065.

(4) Rowe, S. M.; Miller, S.; Sorscher, E. J. *N. Engl. J. Med.* **2005**, *352* (19), 1992–2001.

(5) Riordan; Rommens, J.; Kerem, B.; Alon, N.; Rozmahel, R.; Grzelczak, Z.; Zielenski, J.; Lok, S.; Plavsic, N.; Chou, J.; Et, A. *Science.* **1989**, *245* (4922), 1066–1073.

(6) Smith, S. S.; Steinle, E. D.; Meyerhoff, M. E.; Dawson, D. C. *J. Gen. Physiol.* **1999**, *114* (4), 799–818.

(7) Griesenbach, U.; Alton, E. W. F. W. *F1000Prime Rep.* **2015**, *7*, 64.

(8) Clancy, J. P.; Jain, M. *Am. J. Respir. Crit. Care Med.* **2012**, *186* (7), 593–597.

(9) Quon, B. S.; Rowe, S. M. *BMJ* **2016**, *352*, i859.

(10) Hadida, S.; Van Goor, F.; Zhou, J.; Arumugam, V.; McCartney, J.; Hazlewood, A.; Decker, C.; Negulescu, P.; Grootenhuis, P. D. J. *J. Med. Chem.* **2014**, *57* (23), 9776–9795.

(11) Smith, E.; Collins, I. *Future Med. Chem.* **2015**, *7* (2), 159–183.

(12) Hatanaka, Y.; Hashimoto, M.; Kurihara, H.; Nakayama, H.; Kanaoka, Y. *J. Org. Chem.* **1994**, *59* (2), 383–387.

(13) Alkhouri, B.; Denning, R. a; Kim Chiaw, P.; Eckford, P. D. W.; Yu, W.; Li, C.; Bogojeski, J. J.; Bear, C. E.; Viirre, R. D. *J. Med. Chem.* **2011**, *54* (24), 8693–8701.

(14) Hashimoto, M.; Hatanaka, Y. *European J. Org. Chem.* **2008**, No. 15, 2513–2523.

(15) MacKinnon, A.; Taunton, J. *Curr. Protoc. Chem. Biol.* **2009**, *1* (415), 55–73.

(16) Dubinsky, L.; Krom, B. P.; Meijler, M. M. *Bioorg. Med. Chem.* **2012**, *20* (2), 554–570.

(17) Kumar, N. S.; Young, R. N. *Bioorg. Med. Chem.* **2009**, *17* (15), 5388–5395.

(18) Schneider, E. K.; Huang, J. X.; Carbone, V.; Baker, M.; Azad, M. A. K.; Cooper, M. A.; Li, J.;

Velkov, T. *J. Mol. Recognit.* **2015**, *28* (6), 339–348.

(19) DeMattei, J.; Looker, A.; Neubert-Langille, B.; Truedeau, M.; Roeper, S.; Ryan, M. P.; Dahrika, M.; Guerette, Y.; Krueger, B. R.; Grootenhuis, P. D. J.; Van Goor, F.; Botfield, M.; Zlokarnik, G. Process for making modulators of cystic fibrosis transmembrane conductance regulator. US 8,835,639 B2, 2014.

(20) Eng, J. K.; McCormack, A. L.; Yates, J. R. *J. Am. Soc. Mass Spectrom.* **1994**, *5* (11), 976–989.

(21) The Universal Protein Resource (UniProt) http://www.uniprot.org/uniprot/P02768 (accessed Jan 8, 2018).

(22) Curry, S.; Mandelkow, H.; Brick, P.; Franks, N. *Nat. Struct. Biol.* **1998**, *5* (9), 827–835.

(23) Majorek, K. A.; Porebski, P. J.; Dayal, A.; Zimmerman, M. D.; Jablonska, K.; Stewart, A. J.; Chruszcz, M.; Minor, W. *Mol. Immunol.* **2012**, *52* (3–4), 174–182.

(24) Sugio, S.; Kashima, A.; Mochizuki, S.; Noda, M.; Kobayashi, K. *Protein Eng.* **1999**, *12* (6), 439–446.

(25) Maitra, R.; Sivashanmugam, P.; Warner, K. *J. Biomol. Screen.* **2013**, *18* (9), 1132–1137.

(26) Ahmadi, S.; Bozoky, Z.; Di Paola, M.; Xia, S.; Li, C.; Wong, A. P.; Wellhauser, L.; Molinski, S. V; Ip, W.; Ouyang, H.; Avolio, J.; Forman-Kay, J. D.; Ratjen, F.; Hirota, J. A.; Rommens, J.; Rossant, J.; Gonska, T.; Moraes, T. J.; Bear, C. E. *npj Genomic Med.* **2017**, *2* (1), 12.

(27) Melis, N.; Tauc, M.; Cougnon, M.; Bendahhou, S.; Giuliano, S.; Rubera, I.; Duranton, C. *Br. J. Pharmacol.* **2014**, *171* (15), 3716–3727.

(28) Gottlieb, H. E.; Kotlyar, V.; Nudelman, A. *J. Org. Chem.* **1997**, *62* (21), 7512–7515.

(29) Sheldrick, G. M. *Acta Crystallogr. Sect. A Found. Crystallogr.* **2015**, *71* (1), 3–8.

(30) Sheldrick, G. M. *Acta Crystallogr. Sect. C Struct. Chem.* **2015**, *71* (1), 3–8.

(31) Hübschle, C. B.; Sheldrick, G. M.; Dittrich, B. *J. Appl. Crystallogr.* **2011**, *44* (6), 1281–1284.

(32) Farrugia, L. J. *J. Appl. Crystallogr.* **2012**, *45* (4), 849–854.

(33) Fenn, T. D.; Ringe, D.; Petsko, G. A. *J. Appl. Crystallogr.* **2003**, *36* (3 II), 944–947.

(34) Molinski, S. V; Ahmadi, S.; Hung, M.; Bear, C. E. *J. Biomol. Screen.* **2015**, *20* (10), 1204–1217.

(35) Kalli, A.; Hess, S. *Proteomics* **2012**, *12* (1), 21–31.